Effect of exchangeable cation on the swelling property of 2:1 dioctahedral smectite—A periodic first principle study

Abhijit Chatterjee, Takeo Ebina, Yoshio Onodera, and Fujio Mizukami

Citation: J. Chem. Phys. **120**, 3414 (2004); doi: 10.1063/1.1640333
View online: http://dx.doi.org/10.1063/1.1640333
View Table of Contents: http://jcp.aip.org/resource/1/JCPSA6/v120/i7
Published by the American Institute of Physics.

Effect of exchangeable cation on the swelling property of 2:1 dioctahedral smectite—A periodic first principle study

Abhijit Chatterjee,[a] Takeo Ebina, Yoshio Onodera, and Fujio Mizukami
Laboratory of Membrane Chemistry, National Institute of Advanced Industrial Science and Technology, AIST Tohoku, 4-2-1 Nigatake, Miyagino-ku, Sendai 983-8551, Japan

(Received 23 June 2003; accepted 17 November 2003)

We used both localized and periodic calculations on a series of monovalent (Li^+,Na^+,K^+,Rb^+,Cs^+) and divalent (Mg^{2+},Ca^{2+},Sr^{2+},Ba^{2+}) cations to monitor their effect on the swelling of clays. The activity order obtained for the exchangeable cations among all the monovalent and divalent series studied: $Ca^{2+}>Sr^{2+}>Mg^{2+}>Rb^+>Ba^{2+}>Na^+>Li^+>Cs^+>K^+$. We have shown that, in case of dioctahedral smectite, the hydroxyl groups play a major role in their interaction with water and other polar molecules in the presence of an interlayer cation. We studied both type of clays, with a different surface structure and with/without water using a periodic calculation. Interlayer cations and charged 2:1 clay surfaces interact strongly with polar solvents; when it is in an aqueous medium, clay expands and the phenomenon is known as crystalline swelling. The extent of swelling is controlled by a balance between relatively strong swelling forces and electrostatic forces of attraction between the negatively charged phyllosilicate layer and the positively charged interlayer cation. We have calculated the solvation energy at the first hydration shell of an exchangeable cation, but the results do not correspond directly to the experimental d-spacing values. A novel quantitative scale is proposed with the numbers generated by the relative nucleophilicity of the active cation sites in their hydrated state through Fukui functions within the helm of the hard soft acid base principle. The solvation effect thus measured show a perfect match with experiment, which proposes that the reactivity index calculation with a first hydration shell could rationalize the swelling mechanism for exchangeable cations. The conformers after electron donation or acceptance propose the swelling mechanism for monovalent and divalent cations. [DOI: 10.1063/1.1640333]

1. INTRODUCTION

Clays are lamellar aluminosilicates with a large variety of physicochemical properties, such as swelling, adsorption, surface acidity, ion exchange, etc. Smectites a member of the 2:1 dioctahedral structural unit with one octahedral layer is sandwiched between two tetrahedral layers. Montmorillonite and beidellite are members of the 2:1 dioctahedral smectite family. They share the common feature that two tetrahedral sites sandwich a sheet of octahedrally coordinated metal ion. The substitution of a bivalent metal ion for octahedral aluminum in montmorillonite and the substitution of a trivalent metal ion for tetrahedral silicon in beidellite results in a net negative layer charge, and the interaction with positive ions (exchangeable cation) to form an interlayer hydrated phase. There exists a high repulsive potential on the surface resulting from isomorphous substitution.

Sposito *et al.*[1] pointed out that the OH bond is directed parallel to the clay sheet with the hydrogen pointing to the octahedral vacancy for dioctahedral clays. This OH may act as the active site for molecular adsorption[2] and expected to play a major role in the catalytic activity of 2:1 clays, in their interaction with water and other polar molecules in the presence of an interlayer cation. Hence, it is important to examine the orientation of an exchangeable cation more closely. Interlayer cation and charged clay surfaces interact strongly with polar solvents. As a result, 2:1 clays expand in the presence of water in an aqueous solution. This process is known as crystalline swelling.[3] The extent of swelling is controlled by a balance between relatively strong swelling forces, due to the hydration potential of the interlayer cations, charge sites, electrostatic forces of attraction between the positively charged interlayer cation,[4] and a negatively charged 2:1 phyllosilicate layer. In colloid science,[5,6] the structure of water and the distribution of interlayer cations at the clay–water interface remain topics of great interest. Applying different experimental techniques, Cuardos *et al.*[7] showed that the amount of water adsorbed by smectites is a function of the interlayer cations. The interlayer cation modifies the surface area of the smectite and creates water complexes in the interlayer, which differ either in the number of molecules and/or spatial deposition. A fundamental but unresolved issue is the extent to which interlayer cations were hydrated by water molecules in the 2:1 smectite family.[8–10] The equilibrium hydration state of clay in the regime of interlayer hydrates[11,12] is known to be a function of the magnitude and location of the clay layer charge, the interlayer ion identity, the applied pressure, the temperature, and the water chemical potential, as determined by vapor pressure or solution ionic strength using molecular dynamics. Most of the studies are

[a]Author to whom correspondence to be addressed. Phone: +81-22-237-5211; Fax: +81-22-237-5217; Electronic mail: c-abhijit@aist.go.jp

based on the Monte Carlo (MC) and Molecular dynamics (MD) simulations to understand the swelling of clays or to study the clay–water interface.[13–17] An experimental study probed the influence of layer charge on the hydration of the external surface of expandable 2:1 phyllosilicates.[18] The model assumes that the interlayer volume controls interlayer hydration and the number of cation/charge sites on external surfaces controls the hydration of external surfaces. There is as well a molecular dynamics study for water mobility of bivalent metal cations in case of the beidellite type of clays.[19] Delville[2] has shown that the water molecules form a hydrogen bond with the lone pair of the oxygen at the center of the hexagonal cavity. This is possible for dioctahedral clays, as the proton is directed parallel to the plane of the clay. From electrostatic calculations[20] it has been observed that the orientations of these hydroxyl groups are sensitive to the octahedral cation plane at the center of the clay layer. In our earlier study[21–25] we rationalized the structure property relationship in montmorillonite clays and observed that the hydroxyl groups expected to play a crucial role in the catalytic activity of dioctahedral clays. A recent study of Marry *et al.*,[26] on monohydrated montmorillonite, suggested that Cs^+ diffuse faster than Na^+, and the arrangement of clay surfaces play a significant part in the choice of sites occupied by cations as well in their mobility.

The hard soft acid-base (HSAB) principles classify the interaction between acids and bases in terms of global softness. Pearson proposed the global HSAB principle.[27] The global hardness was defined as the second derivative of energy with respect to the number of electrons at constant temperature and external potential, which includes the nuclear field. The global softness is the inverse of global hardness. Pearson also suggested a principle of maximum hardness (PMH),[28] which states that, for a constant external potential, the system with the maximum global hardness is most stable. In recent days, DFT has gained widespread use in quantum chemistry. Some DFT-based local properties, e.g., Fukui functions and local softness,[29] have already been used for the reliable predictions in various types of electrophilic and nucleophilic reactions in the case of zeolites and clay materials.[30–33]

Numerous theoretical studies have been made on the effect of hydration on the molecular charge distribution of cations, anions, and neutral molecules.[34–36] Mainly, these studies were conducted with Meirtus–Scrocco–Tomasi self-consistent reaction field method. Generally, when compared to a gas phase calculation, the solvent environment alters the charge distribution of a molecule, and there is an increase in the dipole moment of the molecules. In addition, water enhances the intrinsic reactivity of polar molecules toward nucleophilic and electrophilic attack.[34] Based on this, we wish to measure the similar properties for the hydrated cation complexes. We have explored the role of layer charge on the catalytic activity of clay for two different types of smectite and common exchangeable Na^+ with a single water molecule.[25] We have traced the active center of the clay structure with a reactivity index and then placed the cation on both the surfaces with a single water molecule and optimized periodically. It is observed that an interlayer cation (Na^+) has a lesser influence on hydrogen bond formation in the presence of a single water molecule. This encourages us to study the hydrated cations at least at their first layer of hydration, which is explained in detail elsewhere in the relevant part of this article.

The aim of the current paper is to monitor the effect of monovalent and divalent cations on the swelling property of clays. We have studied a range of exchangeable cations. A periodic calculation followed by localized reactivity index study was performed to rationalize the phenomenon in the monolayer hydration scenario. We then extrapolated our scheme to compare the activity of mono- and divalent cations in terms of their swelling phenomenon in the clay interlayer. A rational scale is derived to compare with the experimental order and a plausible explanation for their activity is to be prescribed from the monohydrated configuration of the exchangeable cations.

II. THEORY

In density functional theory, hardness (η) is defined as[37]

$$\eta = 1/2(\delta^2 E/\delta N^2)\,\nu(r) = 1/2(\delta\mu/dN)_\nu,$$

where E is the total energy, N is the number of electrons of the chemical species, and μ is the chemical potential.

The global softness, S, is defined as the inverse of the global hardness, η,

$$S = 1/2\,\eta = (\delta N/\delta\mu)_\nu.$$

Using the finite difference approximation, S can be approximated as

$$S = 1/(\mathrm{IE} - \mathrm{EA}), \tag{1}$$

where IE and EA are the first ionization energy and electron affinity of the molecule, respectively.

The Fukui function $f(r)$ is defined by[29]

$$f(r) = [\delta\mu/d\nu(r)]_N = [\delta\rho(r)/\delta N]_\nu. \tag{2}$$

The function "f" is thus a local quantity, which has different values at different points in the species, N is the total number of electrons, μ is the chemical potential, and ν is the potential acting on an electron due to all nuclei present. Since $\rho(r)$ as a function of N has slope discontinuities, Eq. (1) provides the following three reaction indices:[29]

$$f^-(r) = [\delta\rho(r)/\delta N]_\nu^- \quad \text{(governing electrophilic attack)},$$

$$f^+(r) = [\delta\rho(r)/\delta N]_\nu^+ \quad \text{(governing nucleophilic attack)},$$

$$f^0(r) = 1/2[f^+(r) + f^-(r)] \quad \text{(for radial attack)}.$$

In a finite difference approximation, the condensed Fukui function[38] of an atom, say x, in a molecule with N electrons, are defined as

$$\begin{aligned} f_x^+ &= [q_x(N+1) - q_x(N)] \quad \text{(for nucleophilic attack)},\\ f_x^- &= [q_x(N) - q_x(N-1) \quad \text{(for electrophilic attack)},\\ f_x^0 &= [q_x(N+1) - q_x(N-1)]/2 \quad \text{(for radical attack)}, \end{aligned} \tag{3}$$

where q_x is the electronic population of atom x in a molecule.

The local softness $s(r)$ can be defined as

$$s(r)=(\delta\rho(r)/\delta\mu)_v. \tag{4}$$

Equation (3) can also be written as

$$s(r)=[\delta\rho(r)/\delta N]v[\delta N/\delta\mu]_v=f(r)S. \tag{5}$$

Thus, local softness contains the same information as the Fukui function $f(r)$ plus additional information about the total molecular softness, which is related to the global reactivity with respect to a reaction partner, as stated in the HSAB principle. Atomic softness values can easily be calculated by using Eq. (4), namely,

$$\begin{aligned} s_x^+ &= [q_x(N+1)-q_x(N)]S, \\ s_x^- &= [q_x(N)-q_x(N-1)]S, \\ s_x^0 &= S[q_x(N+1)-q_x(N-1)]/2. \end{aligned} \tag{6}$$

III. COMPUTATIONAL METHODOLOGY AND MODEL

The software package CASTEP (Cambridge Serial Total Energy package), which has been described elsewhere[39,40] and associated programs for symmetry analysis were used for the calculations. CASTEP is a pseudopotential total energy code that employs Perdew and Zinger[41] parametrization of the exchange-correlation energy, super cells and special point integration over the Brillouin zone, and a plane wave basis set for the expansion of the wave functions. The methodology has been used in mineralogy to examine the hydration of corderite.[42] Becke–Perdew parametrization[43,44] of the exchange-correlation functional, which includes gradient correction (GGA), was employed, as this is a well-established technique.[45,46] The pseudopotentials are constructed from the CASTEP database. The screening effect of core electrons is approximated by LDA, while the screening effect for valence electrons is approximated by GGA. This is a reasonable approximation, as shown by Garcia *et al.*[47] To obtain equilibrium structures for a given set of lattice constants, ionic and electronic relaxations were performed using the adiabatic or ''Born–Oppenheimer'' approximation, where the electronic system is always in equilibrium with the ionic system. Relaxations were continued until the total energy had converged. In the present calculations, kinetic cutoff energies between 600 and 1500 eV have been used. The Monkhorst–Pack scheme[48] was used to sample the Brillouin zone. The calculations were restricted to one special K point in the Brillouin zone, placed at (0.0,0.0,0.0).

In the present study, all calculations have been carried out with DFT[49] using the DMOL^3 code of Accelrys Inc. A gradient corrected functional BLYP[50,51] and DNP basis set[52] was used throughout the calculation. Basis set superposition error (BSSE) was also calculated for the current basis set in a nonlocal density approximation (NLDA) using the Boys–Bernardi method.[53] Single-point calculations of the cation and anion of each molecule at the optimized geometry of the neutral molecule were also carried out to evaluate Fukui functions, global and local softness. The condensed Fukui function and atomic softness were evaluated using Eqs. (3) and (6), respectively. The gross atomic charges were evaluated by using the technique of electrostatic potential (ESP) driven charges.

The ideal formula of the clay montmorillonite, a member of the 2:1 dioctahedral smectite family, is $(M_x^+[Si_aAl_{8-a}]Al_bM_{g4-b}O_{20}(OH)_4$,[54] where $x=(12-a-b)$ is the layer charge, and the M is the balancing cation either monovalent or divalent. The desired structures of montmorillonite and beidellite have been generated from the structure of well-defined pyrophillite.[55] They are having the formula $MSi_8Al_3MgO_{20}(OH)_4$ and $MAlSi_7Al_4O_{20}(OH)_4$, respectively. Hydrated phase calculations were performed with the minimum energy structures of the clays at the unhydrated phase. The interlayer structure was held fixed and the interlayer spacing was increased to accommodate the water molecule. Unhydrated respective clay structures were minimized using two steps: (1) the tetrahedral layers were allowed to relax whereas octahedral ions were kept fixed, and (2) all the ions were relaxed simultaneously relative to a fixed octahedral ion (magnesium or aluminum) until the total energies were converged. In both steps the interlayer cation is relaxed. For the hydrated phases we relaxed the cation water and the interlayer space; the lower part of the structure was kept fixed to compromise between CPU cost and accuracy.

The water complexes for the individual cations were generated from the optimized periodic structure. The geometries of the localized cations were isolated and then relaxed again for each neutral cationic and anionic form for the calculation of reactivity indices.

IV. RESULTS AND DISCUSSION

So far we have seen both form theoretical and experimental work of different groups that the interlayer water orientation depends mainly on cation location; if it lies closer to the clay layers the interlayer is weakly influenced by these cations, whereas for other sets of cations the degree of hydrogen bonding among a water molecule is greater as the cation stays away from the clay layer. Delville *et al.*[2] have shown that the factor responsible for swelling is not enthalpy but entropy. The activity of the compensating cation is zero in the bulk water and positive in the clay suspension. The cations must move from the clay suspension to the bulk water to equalize their activity. Again the solvation interaction is short-range interaction. In clay swelling there exists two kinds of water molecule: one bonded to an interlayer cation in its hydration shell and another the nonbonded water laying as the bulk. Therefore, to rationalize the swelling phenomenon, one needs to play with the water molecules present in the hydration shell. There is a consensus to the fact that clay swelling is dependent on humidity. Because of the increase of higher humidity, the hydration layer will increase, and after reaching three-layer hydration it will saturate, and any further addition of water does not modify either the hydration shells of the clay surface or the interlamellar cations. Therefore we need to check the role of the cation location on the hydration process, and we limited the calculation to a first hydration shell with a strong short-range interaction. If

TABLE I. The ionic radii, *d* spacing, and number of water layer present during hydration as observed from experiment.

Exchangeable cations	Ionic radii in Å	*d* spacing in Å measured by XRD	Number of water layers
Li	0.76	12.5	1
Na	1.02	12.5	1
K	1.38	12	0.42
Rb	1.52	12.8	1
Cs	1.67	12.47	1
Mg	0.72	14.5	2
Ca	1.00	15	2
Sr	1.18	14.9	2
Ba	1.35	12.5	1

this can be modeled accurately, then we can extrapolate the situation for the cases with a higher hydration shell. Localized information then can tell us the activity of the cation after first hydration and as well its aptitude for further hydration. This is followed by a localized reactivity index calculation, which can quantitatively predict the activity of the cations before and after hydration. This will help us to propose their further hydration/catalytic activity at larger hydration as well.

A. Experimental parameters as known

A comparative list of properties of the exchangeable cations as obtained from experiment[7] was tabulated in Table I. There is an increase in the ionic radii for both the monovalent and divalent cations down the group, as expected. We have shown these numbers to question ourselves as to whether the ionic radii has any contribution on the swelling phenomenon or, in other words, do the ionic radii dictate the number of water molecules around the cations. By combining the trend for both a mono- and divalent cation in terms of the ionic radii, the exchangeable cations fall in the order $Cs^{+}>Rb^{+}>K^{+}>Ba^{+2}>Sr^{+2}>Na^{+}>Ca^{+2}>Li^{+}>Mg^{+2}$.

The *d* spacing is the distance between the adjacent silica layers to the bottom silica layer of a smectite species, as shown in Fig. 1, and generally there is a marked difference

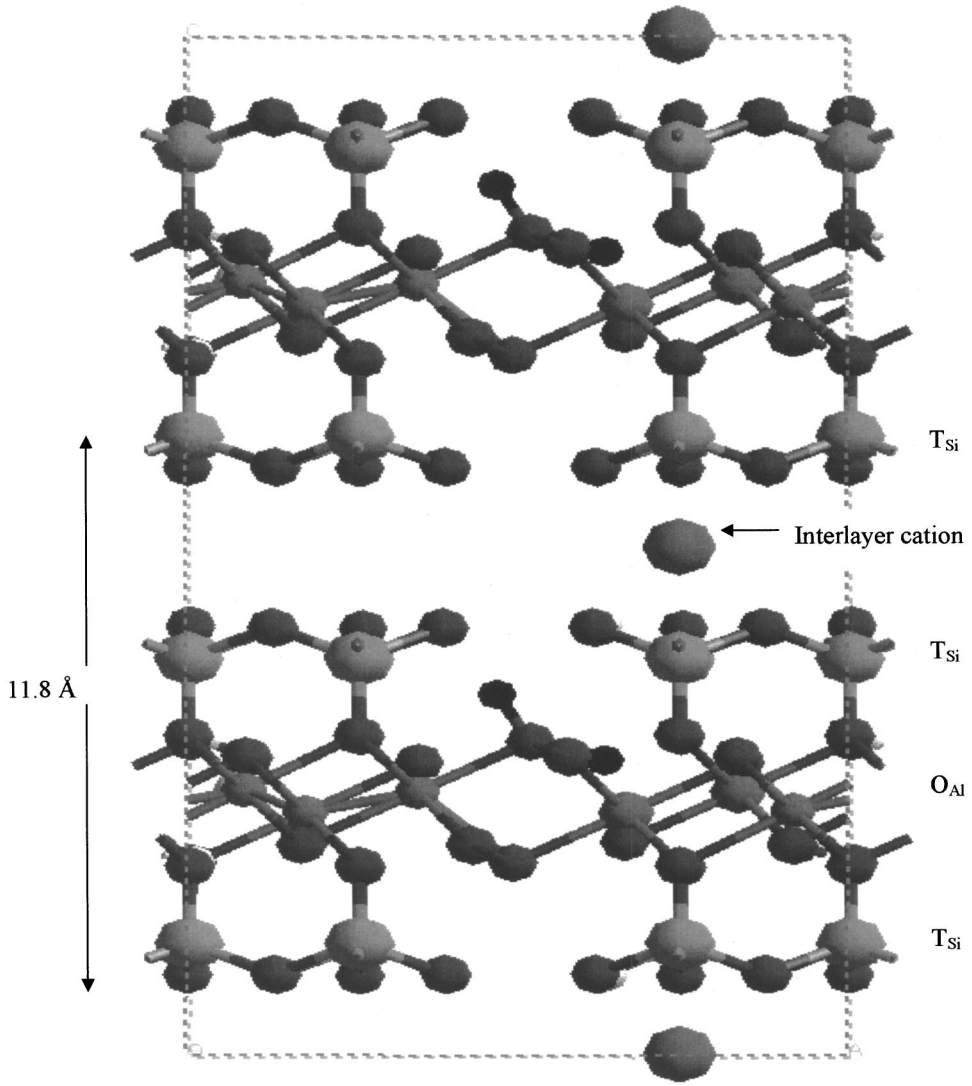

FIG. 1. Model of 2:1 dioctahedral clay structure with interlayer cation and the layers present labeled to show the *d* spacing. T_{Si}=tetrahedral silicon; O_{Al}=octahedral aluminum.

of *d* spacing between a monovalent and divalent cation. It is also seen that for the bivalent cations, the number of water layers is 2 in comparison to 1 for the monovalent cations at a fixed humidity of 30%. The clay layer spacing increases more in the case of a divalent cation than that of a monovalent cation, with the exception of Ba^{+2}. Experimentally, it is also observed that the *d* spacing is related to the number of water layers surrounding the exchangeable cation. For K^+, the *d* spacing after swelling is lowest and the number of water layers is least (Table I). We have also seen that, except Ba^{2+}, all other bivalent metal cations are surrounded by a two-water layer at that specific *d* spacing. Depending on the extent of increment in basal spacing [as observed from the x-ray diffraction experiments (Table I)] between two smectite sheets, two types of swelling mechanism are proposed;[56] (1) crystalline swelling and (2) osmotic swelling. Crystalline swelling occurs for monolayer water adsorption around the cation, held by hydrogen bonding to the hexagonal network of oxygen atoms. This could result in an increase of *d* spacing in the range of about 10–20 Å. The osmotic swelling is the phenomenon when interlayer spacing increases abruptly to 30–40 Å with the water content due to the interaction of the layers; this is beyond the scope of this study. We therefore concentrated on monolayer hydration to compare the localized structure surrounding a mono- and divalent cation.

B. Periodic calculation to validate the model and to monitor the effect of layer charge on cation location

With this experimental background we planned the periodic calculation to proceed through the following path: (1) to compare the role of layer charge on binding the cation in the interlayer surface, the location of the exchangeable cation in unhydrated form over both of the chosen smectite; (2) from the results we then need to monitor the influence of hydration on the location of the cation at their hydrated phase.

We have chosen the model of the montmorillonite- and beidellite-type clays with structural formula $MSi_8Al_3MgO_{20}(OH)_4$ and $MAlSi_7Al_4O_{20}(OH)_4$, respectively, and optimized the structure in their unhydrated form. The internal coordinates matches with the available experimental values. The deviation is mostly at the basal oxygen atoms of the tetrahedral layer, due to the rotation of the SiO_4 tetrahedral by 13.2° and a tilt by 4.6°, on average. This is in close agreement with the numbers generated by Bridgeman *et al.*[57] with a rotation of 18.4° and a tilt of 6.5°. It is observed that for montmorillonite the hydroxyl hydrogen attached with the octahedral aluminum makes an angle of 24.12° with an *a*-*b* plane, which is in close agreement with the observation of Giese *et al.*[20] They predicted the angle to be 26° by minimizing the electrostatic energy of pyrophyllite with respect to the hydroxyl hydrogen. There is no available data for beidellite to compare.

It is known that the long range swelling in the clays is mainly due to the electrostatic repulsion between the clay sheets bearing the same charge. But this view neglects the role of exchangeable cations present in the interlayer. We have to consider the charged surface plus the counter ions as a whole. So here we try to figure out the dependence of the location of a cation on the layer charge originated from the octahedral/tetrahedral substitution in the specific clay structure. First we studied montmorillonite, where the octahedral aluminum is replaced by magnesium, resulting in a negative charge to be balanced by an exchangeable cation. To test the effect of layer charge, we placed the Na^+ at a starting distance of 2.5 Å with hydroxyl hydrogen attached to octahedral magnesium and then optimized the cation at different distances from the chosen center. We have compared this situation with beidellite, in which the distance between the cation and the hydroxyl hydrogen attached with unsubstituted octahedral aluminum is varied and the energy is plotted against the distance between a cation and the hydroxyl hydrogen, as shown (Fig. 2). For montmorillonite, the cation gets stabilized at a distance of 2.8 Å from the hydroxyl hydrogen, which closely resembles our earlier finding that the cation to magnesium distance is 3.5 Å.[25] For beidelite, there is almost no role of hydroxyl hydrogen attached with the octahedral center on the adsorption process. To monitor the influence of the layer charge generated from tetrahedral substitution, the cation is placed on top of the surface hydrogen over the beidellite model. The situation is compared with montmorillonite, where there is no tetrahedral substitution. The energy was again plotted with the distance between the cation and surface hydrogen (Fig. 3). Figure 3 shows that in case of montmorillonite the surface hydrogen have no contribution on the adsorption process, as expected. The cation stabilized in beidellite over the tetrahedral-substituted site at a distance of 1.8 Å from the surface hydrogen closely

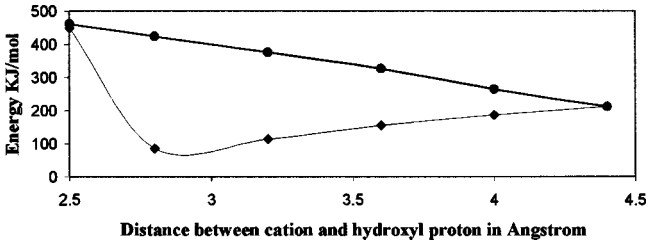

FIG. 2. Potential energy curve to study the feasibility of interaction between the exchangeable cation and the clay structure, in terms of the distance between cation and the hydroxyl hydrogen present in both montmorillonite (♦) and beidellite (●).

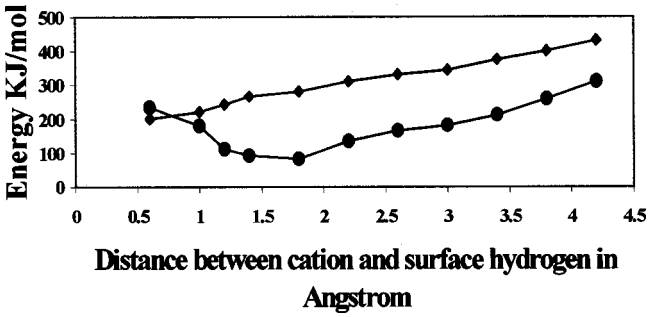

FIG. 3. Potential energy curve to study the feasibility of an interaction between the exchangeable cation and the clay surface, in terms of the distance between the cation and the surface hydrogen present in both montmorillonite (♦) and beidellite (●).

matches with our prior findings[25] with sodium, where the Na–Al distance was 2.8 Å. The results show that the location of the cation is influenced by the source of the layer charge. When the layer charge is originated from the substitution of octahedral aluminum, the hydroxyl hydrogen shows an inclination to stabilize the cation and the cation stays on top of it with a larger distance form the center of the layer charge; whereas when the layer charge is originated from the tetrahedral substitution at the tetrahedral silicon, then the cation is more favorably interacted with surface hydroxyl. It also shows that the distance between the cation and surface hydroxyl is less, compared to the other, pointing to a restricted swelling phenomenon. It also proposed that in the case of montmorillonite-type clay we might find a better H-bonding phenomenon among the water molecules interacting in the presence of the cation. These results match with the MD results,[11] suggesting that the *d* spacing for beidellite will be smaller than that of Na montmorillonite, as most of their structural charges reside in the tetrahedral sheet, causing stronger interlayer electrostatic forces.

C. Periodic calculation to locate the unhydrated and hydrated exchangeable cation in montmorillonite

In natural clay (bentonite), montmorillonite is the main constituent. We have as well observed from the results of an earlier section that due to a different layer charge source, the cation location is influenced, and the cation will have much mobility in montmorillonite than beidellite, hence we decided to explore montmorillonite more carefully. We therefore first optimized the montmorillonite structure with different exchangeable cations, both monovalent and divalent. Then we added water around the cation center until its first solvation shell. We have calculated the solvation energy and further monitored the cell parameters after hydration to rationalize the swelling phenomenon. We have concentrated only on the first shell of solvation to visualize the effect of hydration on the swelling phenomenon. This is because it is observed that in the swelling process each cation is first hydrated to its first hydration shell; the further increment is dependent on the amount of humidity. The first layer therefore will be the best choice to explore the electronic phenomenon occurring involving a cation and the clay interface. The model of multilayer solvation is shown in Fig. 4 to have a feeling of the process; only the hydrated water is shown for visual clarity. The first hydration shell is as well can be the shell to look at the interwater H-bonding process, which may be pronounced or suppressed, depending on the location of the cation over the clay surface. The increase in humidity does not favorably increase the layers around the cation; the water then may reside as a nonbonded molecule in the bulk, and does not contribute much toward the swelling phenomenon.

For the optimization of a montmorillonite structure with a series of monovalent and divalent cations, we relaxed the cation, the top tetrahedral silicon layer, and the octahedral aluminum/magnesium layer; the bottom two layers were kept fixed throughout the calculation. The results are shown in Table II and the idealized cell parameters for the structure are given at the top of Table II. After analyzing the results, we find that monovalent cations do not show any regular trend and all the parameters fluctuating bit randomly; whereas for the bivalent cations parameter, *a* is decreasing and *c* is increasing through the group. Irrespective of the amount of charge on the cation, in all cases the exchangeable cation lies on top of the hydroxyl hydrogen.

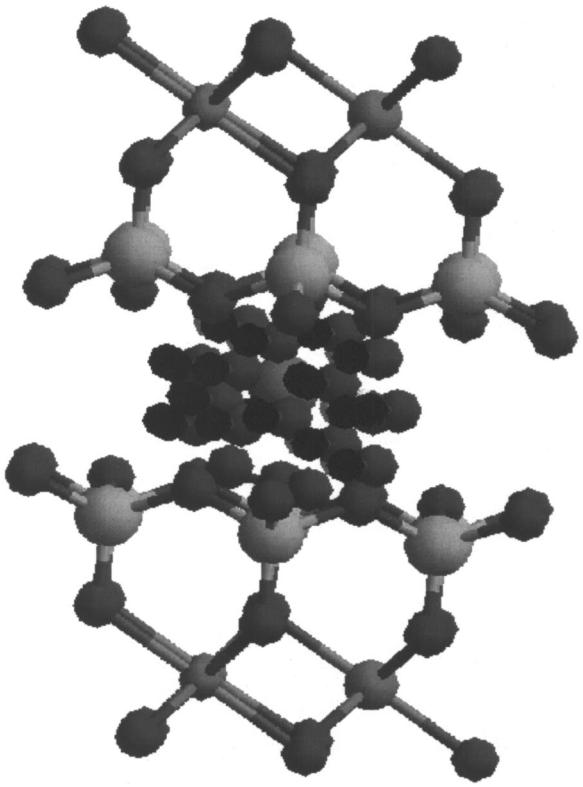

FIG. 4. Model of the montmorillonite clay structure with multiplayer hydration around the exchangeable cation.

In each optimized structure water was added around each cation. A constraint in terms of the radius of the cation water complex has been imposed to consider only the first hydration shell of the cation. We have made a cavity of 2 Å around the cation This distance has been chosen based on our earlier localized cluster calculation results,[25] where we have seen that for sodium, water molecules reside within that radius. The model over which we are adding this water is montmorillonite; hence the cation is located on top of hydroxyl hydrogen, where the cation–Mg distance is 3.5 Å.

TABLE II. The cell parameter for the optimized structure of montmorillonite with different mono and divalent cations without hydration. Original cell parameter: $a=5.15$ Å, $b=8.90$ Å, $c=9.59$ Å, $\alpha=90°$, $\beta=100°$, and $\gamma=90°$.

Metal	*a*	*b*	*c*	α	β	γ
Li	5.129	8.877	10.900	89.96	99.11	89.94
Na	5.145	8.946	10.533	90.22	97.58	89.97
K	5.121	8.906	10.797	89.98	98.92	89.93
Rb	5.165	8.896	10.146	89.98	96.95	90.92
Cs	5.134	8.857	10.971	89.94	98.94	89.96
Mg	5.167	8.890	10.192	89.84	97.85	89.91
Ca	5.142	8.956	10.552	89.99	99.50	89.96
Sr	5.131	8.950	10.685	90.02	99.40	89.93
Ba	5.128	8.913	10.913	89.99	98.91	89.94

TABLE III. The cell parameter for the optimized structure of montmorillonite with different mono- and divalent cations with hydration. Original cell parameter: $a=5.15$ Å, $b=8.90$ Å, $c=9.59$ Å, $\alpha=90°$, $\beta=100°$, and $\gamma=90°$.

Metal	a	b	c	α	β	γ
Li	5.147	8.923	11.998	90.27	96.79	90.22
Na	5.193	8.992	11.862	89.96	97.01	90.45
K	5.155	8.988	10.338	90.49	98.15	90.09
Rb	5.157	8.986	11.330	89.88	96.35	90.45
Cs	5.140	8.870	11.684	90.47	98.14	90.03
Mg	5.197	8.994	10.662	90.16	97.11	90.65
Ca	5.166	8.998	11.911	91.08	98.98	90.08
Sr	5.156	8.943	11.121	90.39	98.57	90.01
Ba	5.140	8.899	11.614	90.17	98.56	90.23

TABLE IV. Solvation energy in KJ/mol for the monovalent and divalent exchangeable cation after solvation using periodic calculation.

	Total energy in kJ/mol		
Cation	Clay water complex	Clay unit cell + n number of water molecule	Solvation energy (kJ/mol)
Li	−12 298.5	−12 296.27	2.23
Na	−13 432.2	−13 427.05	5.15
K	−12 901.4	−12 899.85	1.55
Rb	−12 312.1	−12 309.55	2.55
Cs	−12 674.1	−12 670.58	3.52
Mg	−12 947.2	−12 945.11	2.09
Ca	−13 003.5	−12 999.41	4.09
Sr	−12 827.8	−12 825.21	2.59
Ba	−12 700.9	−12 697.81	3.09

Our aim is to see the number of water molecules in the first hydration shell. We have added a water molecule around the cation and optimize the structure with the water, cation, and the top two layers to calculate the relative stabilization energy. Water molecules were added until the stabilization energy is constant, to propose the maximum number of water molecules to reside in the first hydration shell is reached. For monovalent cations the number of water molecules surrounding the cations is 5 and that for bivalent cations is 3 in the first hydration shell, as observed at the forced boundary condition. This result matches with our earlier GCMC simulation[25] and as well it matches with the results of Delville *et al.*[2] This as well matches with the experiment in terms of the first hydration layer. It is observed that a bivalent metal like calcium gets sandwiched between two layers of water molecules with each layer consisting of three water molecules. So our calculation reproduces one of the layers of water, which is acting as the first hydration shell.

The cell parameters of the hydrated cations are shown in Table III. The general trend exhibits that, for all the cases there is a swelling along the c direction after hydration, except for potassium. This can be explained by the fact that, in these types of clays one tetrahedral sheet of one unit layer is adjacent to another tetrahedral sheet of another layer. The oxygen atoms here are opposite to one another and the bonding between the layers is weak. Also, there exists a high repulsive potential on the surface of layers resulting form isomorphous substitution. These factors contribute to the increase of the unit cell in the c direction due to the penetration of water. We observe a general increase in the cell parameters after hydration for almost all of the exchangeable cations, comparing the two datasets presented in Table II and Table III for monovalent and divalent cations before and after hydration. Now, in the experiment, the d spacing reported after swelling is for a humidity condition in which there exists multilayers of water for bivalent metal cations; we therefore can not correlate the swelling in numbers with one hydration shell. At this point we calculated the solvation energy for each cation after hydration. The solvation energy is calculated as follows:

$$E_{\text{Solvation}} = E_{\text{Clay water complex}} - [E_{\text{Clay unit cell}} + n \times E_{\text{Water molecule}}],$$

where n is the number of water molecules optimized around a cation over the clay unit cell. The energy of water molecules has been calculated (Table IV) using the same periodic condition as imposed for the clay unit cell. The results show that solvation energy is highest for the solvated sodium cation and smallest for the potassium cation. The values indicate the stability of the water complex around the cation. Calcium shows a perspective second value in that order though it contains a lesser number of water molecules around itself. We therefore cannot see any pronounced difference between the monovalent and divalent cation to account for the difference in swelling phenomenon. Only we can tell that the results have a partial match with experimental findings, and can reproduce the lowest expansion of potassium as observed very well by the experiment. This shows that the bulk calculation is unable to match the experimental trend of swelling. The short-range forces cannot be well depicted by the periodic calculation, which is more concentrated on long-range interactions. The swelling of the clay layers will be observed with a match with experiment if we do a multilayer hydration calculation. This is a very complicated and costly calculation with nonbonded water molecules coming in the picture. From the current results we see that the cations get a favorable bonding with the first hydration shell water, but we were unable to predict the further hydration, or, in other words, we were unable to see the activity of the cations after first hydration, from which we can propose their further hydration. Hence, it seems that it will be nice and cost effective to monitor the localized water environment around the cation, which may then be able to reproduce the experimental trend and as well can foresee the mechanism of multilayer formation for a specific exchangeable cation. We need to answer the following question; why one set of cation (bivalent) has shown increased swelling at the same humidity when the other cation (monovalent) cannot. The different cation must have different affinity and activity to get itself bonded with a certain number of water molecules locally around itself.

D. Hydration or water complexation and elucidation of the phenomenon by reactivity index calculation

With the periodic calculation we have seen that the results with one layer of hydration was unable to correlate the

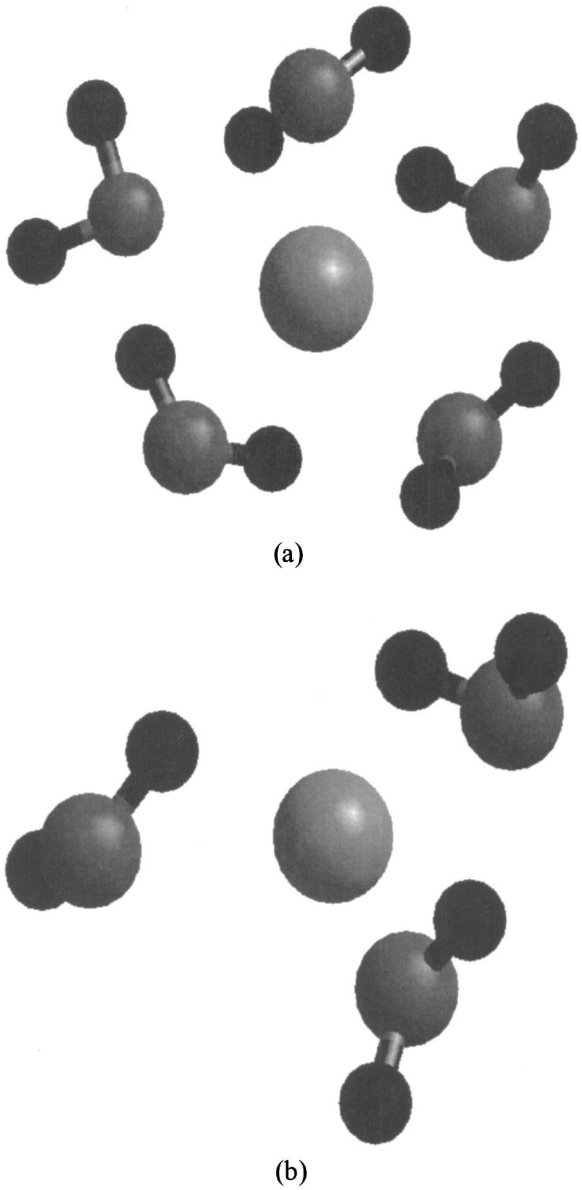

FIG. 5. (a) The model for a monovalent cation hydrated complex with five water molecules as obtained from a periodic calculation using CASTEP; (b) the model for a divalent cation hydrated complex with three water molecules as obtained from a periodic calculation using CASTEP.

swelling phenomenon in terms of *d* spacing. We therefore have started with the cation water complexes for each monovalent and divalent cation to emphasize their localized environment. The models representing the monovalent cation with five water molecules and for a divalent cation with three water molecules is shown in Figs. 5(a) and 5(b), respectively. The global softness of the water complexes of the different cations studied is shown in Table V. As expected, the global softness does not provide a better insight into the understanding, as we have not seen any clear order in the activity of these complexes. Then we have calculated the Fukui function and local softness for each and individual atom centers. The values are given in Table V. For a few cases the Fukui functions and as well the softness values are very close. So it would be difficult to formulate a trend, as our aim is to figure out the possibility of short-range bonding of the cation with water and intermolecular H bonding between water molecules to identify a trend. It, therefore, seems to be a nice idea to calculate the ratio of s_x^+ and s_x^-, termed relative electrophilicity or nucleophilicity. The idea of relative nucleophilicity/electrophilicity was first proposed by Roy *et al.*[58] to predict intramolecular and intermolecular reactivity sequences of carbonyl compounds. This is the ratio of electrophilicity and nucleophilicity of a particular atom center. We have used a similar ratio for the first time to find the best dioctahedral smectite for nitrogen heterocyclic adsorption[59] as well as for the adsorption property of para- and meta-substituted nitrobenzene.[60] The results of relative nucleophilicity s_x^+/s_x^- and electrophilicity s_x^-/s_x^+ were shown in Table V as well. The results show a very clear trend in terms of the activity of the individual cation centers after the hydration and matches with the trend observed by the experiment in terms of *d* spacing after swelling. Here the relative nucleophilicity of potassium is lowest to show that potassium might act as a swelling inhibitor. The findings are similar with the Monte Carlo simulation results of Bock *et al.*[18] They proposed that K^+ ions present in clay as an exchangeable cation acts as a clay swelling inhibitor. As they found that Li^+ or Na^+ can become hydrated and can detach from the surface after hydration, K^+ ions migrate to and bind to the clay surface during simulation. Hence the localized environment of cations after hydration has a marked influence on their reactivity.

TABLE V. The Global softness, Fukui function, local softness, relative nucleophilicity, and relative electrophilicity for the hydrated structure of the exchangeable mono- and divalent cation using ESP charges calculated by DFT.

Cation	Global softness (a.u.)	f_x^+	s_x^+	f_x^-	s_x^-	s_x^+/s_x^-	s_x^-/s_x^+
Li	1.56	0.56	0.87	0.023	0.037	23.51	0.042
Na	1.23	0.83	1.02	0.023	0.028	36.42	0.027
K	1.37	0.81	0.71	0.210	0.290	2.41	0.410
Rb	1.08	0.59	0.64	0.015	0.017	37.64	0.260
Cs	1.11	0.05	0.06	0.003	0.004	18.15	0.050
Mg	2.17	0.78	1.69	0.020	0.044	38.40	0.026
Ca	2.59	0.94	2.45	0.010	0.040	51.68	0.020
Sr	2.39	0.99	2.36	0.025	0.059	39.59	0.024
Ba	2.46	0.42	1.03	0.011	0.028	36.78	0.027

Now, with the numbers in hand it would be nice to see the conformations of each cation water complex to monitor the influence of electron addition/removal. The water cation complex was optimized when neutral, then adding one electron and finally removing one electron from the mother complex the single-point energy was calculated. The conformers at their optimized geometry when neutral, cationic, and anionic are shown in Figs. 6 and 7 for the monovalent cation–water complex and divalent metal cation–water complex, respectively. These figures represent the situation with monovalent sodium and divalent calcium, respectively, as a representative for their group. It can be seen from Fig. 6 that the electron accepting process allows the central cation (sodium) much wider room or flexibility, whereas during electron donation the conformation is quenched and room for

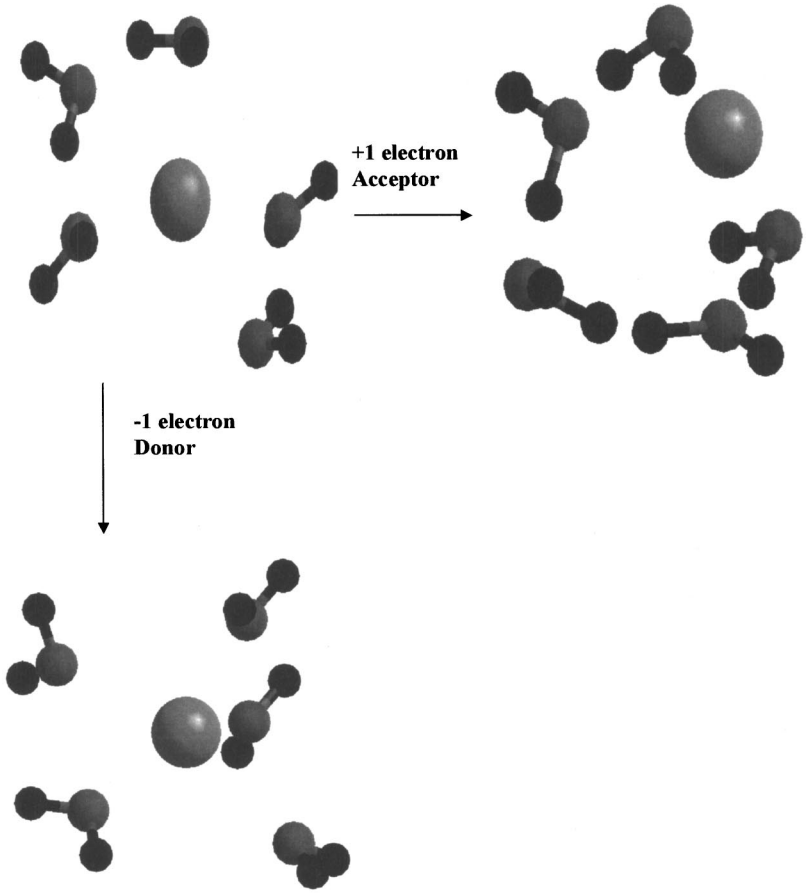

FIG. 6. Schematic representation along with the optimized conformers for a neutral, cationic, and anionic structure for the monovalent hydrated complex.

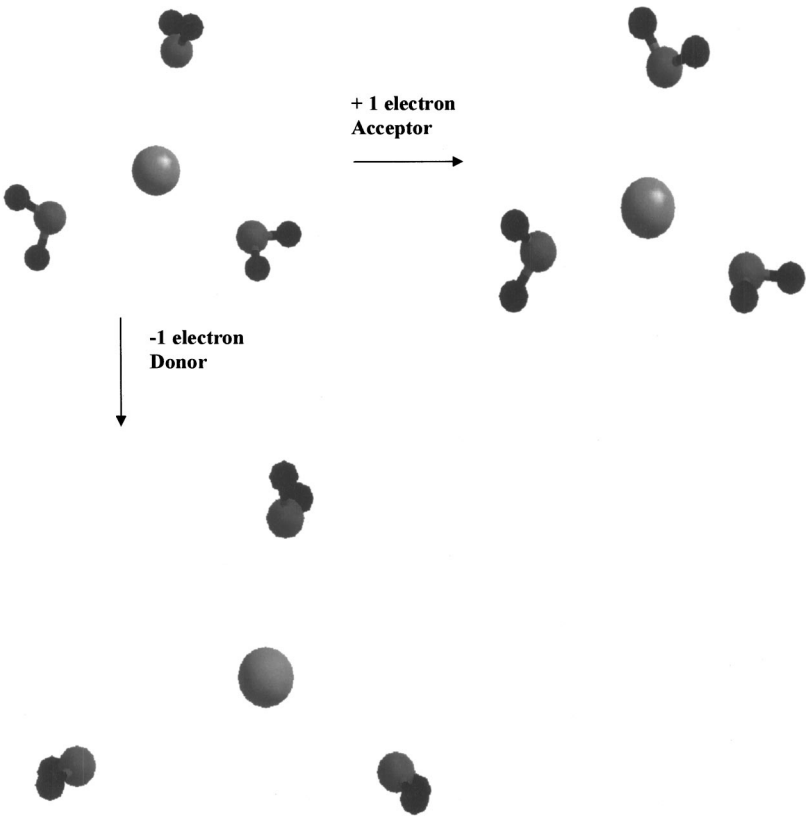

FIG. 7. Schematic representation along with the optimized conformers for a neutral, cationic, and anionic structure for the divalent hydrated complex.

further hydration looks costlier energetically. We therefore propose that the monovalent cation center may undergo monolayer hydration easily and after hydration as well it may still accept electrons to some extent whereas electron donation looks improbable. In the case of a divalent center (here calcium) as shown in Fig. 7, the conformation flexibility is just opposite; when it accepts an electron it remains close to the earlier geometry, whereas the feasibility increases in the case of an electron donating phenomenon. But in both cases there is room for electron acceptance and donation. The feasibility of an electron donating phenomenon justifies further hydration behavior for divalent cation centers. This validates the experimental results about the favorability of bilayer hydration for divalent metal cations at the same humidity criteria. The localized phenomenon can therefore resolve the issue of activity of exchangeable cations. For monovalent cation after the first hydration, the mobility of cation decreases to hinder the bilayer formation,[19] which is opposite for the divalent metal cation.

In this context we wish to refer to two very interesting papers using *ab initio* molecular dynamics method for Li[61]- and Na[62]-type clays. We have seen that the localized reactivity index can predict the activity of these cations for further hydration or catalytic activity from the electron donor acceptor capability. The DFT results as well can successfully postulate the swelling mechanism in terms of the localized hydrogen-bonding scenario. The *ab initio* molecular dynamics may then be able to be used to figure out the liquidlike relaxation dynamics of the second layer to propose a true scenario of the swelling phenomenon.

E. The correlation observed and proposition of a qualitative scale

Here we list the correlation observed in all the abovementioned sections. First, with ionic radii we have observed that the order of radii for the cations is

$$Cs^+ > Rb^+ > K^+ > Ba^{2+} > Sr^{2+} > Na^+ > Ca^{2+} > Li^+ > Mg^{2+}.$$

It is observed that the *d* spacing has a significant variation for a mono- and divalent cation at the same humidity level. The order with experimentally observed *d* spacing is as follows:

$$Ca^{2+} > Sr^{2+} > Mg^{2+} > Rb^+ > Ba^{2+} = Na^+ = Li^+ > Cs^+ > K^+.$$

Now, as three values of the above order are the same, we derived two separate orders for monovalent and divalent cations, respectively,

$$Rb^+ > Na^+ = Li^+ > Cs^+ > K^+;$$

$$Ca^{2+} > Sr^{2+} > Mg^{2+} > Ba^{2+}.$$

Swelling is observed along the *c* parameter of the unit cell for monolayer hydration in case of all the cations studied in general. We therefore calculated the percent expansion and figured out an order for that expansion, which is as follows:

$$Ca^{2+} > Na^+ > Rb^+ > Li^+ > Cs^+ > Ba^{2+} > Mg^{2+} > Sr^{2+} > K^+.$$

The individual order for mono- and divalent cations are as follows:

$$Na^+ > Rb^+ > Li^+ > Cs^+ > K^+ \quad \text{and} \quad Ca^{2+} > Ba^{2+} > Mg^{2+} > Sr^{2+}.$$

Solvation energy, as well, has been calculated for each of the water complexes studied with individual monovalent or divalent cations. The combined order observed is as follows:

$$Na^+ > Ca^{2+} > Cs^+ > Ba^{2+} > Sr^{2+} > Rb^+ > Li^+ > Mg^{2+} > K^+.$$

The order for the group of mono- and divalent cations is as follows:

$$Na^+ > Cs^+ > Rb^+ > Li^+ > K^+ \quad \text{and} \quad Ca^{2+} > Ba^{2+} > Sr^{2+} > Mg^{2+}.$$

The relative electrophilicity and nucleophilicity for the individual hydrated cations were calculated for a better correlation. The order of relative nucleophilicity only is compared, The order is

$$Ca^{2+} > Sr^{2+} > Mg^{2+} > Rb^+ > Ba^{2+} > Na^+ > Li^+ > Cs^+ > K^+,$$

while the order for the individual group of cations is

$$Rb^+ > Na^+ > Li^+ > Cs^+ > K^+ \quad \text{and} \quad Ca^{2+} > Sr^{2+} > Mg^{2+} > Ba^{2+}.$$

The results show that they are a match with the experimental order of *d* spacing. This tells us that the localized reactivity index calculation can propose the swelling phenomenon in a quantitative extent. This also validates that the exchangeable cations at their first hydration shell can reproduce the scenario of clay swelling.

V. CONCLUSION

A very systematic and exhaustive study to rationalize the swelling phenomenon of the clay structure and the influence of monovalent and divalent cations on the swelling property has been performed. Experimentally, it was observed that the monovalent and divalent cations have a marked difference in their swelling capability in terms of *d* spacing without much influence from ionic radii. The exchangeable cation position is located with respect to the location of layer charge to validate our model. The role of layer charge on the location of cations is tested. Due to the availability of montmorillonite in the natural soil we performed the rest of the study with that variety only. Then periodic calculation was performed on the clays to compare the electronic structure before and after hydration. After hydration, swelling of the clay structure in the *c* direction is observed. The solvation energy was calculated, but the trend does not resolve the experimental trend. This is possible because we are only considering one layer of hydration, whereas the experimental trend is

with multilayer hydration as well. Short-range interactions may be the driving force to dictate the swelling phenomenon and not the long-range force. Hence, we tried to test whether a localized calculation can have some answer in terms of the activity of different cations. This allows us to perform a localized reactivity index calculation over the hydrated exchangeable cation. The relative nucleophilicity was used to compare the activity of the cations and a quantitative scale is proposed that matches with the experimental trend in terms of *d* spacing. The activity order for the exchangeable cations among all the monovalent and divalent series studied: $Ca^{2+} > Sr^{2+} > Mg^{2+} > Rb^{+} > Ba^{2+} > Na^{+} > Li^{+} > Cs^{+} > K^{+}$. This is with monohydration only. At the same time from the molecular conformations, we can say that the structural change associated with electron addition (acceptor) and electron subtraction (donor) can rationalize the mechanism for swelling, as these conformers can tell whether one cation can feasibly attempt for multiplayer hydration or not. This is the first time the swelling phenomenon of clays is addressed in electronic level and with high accuracy. Therefore we now can design the material with a different cation depending on their swelling characteristic with a specific target catalytic reaction.

ACKNOWLEDGMENTS

A part of this study was financially supported by the Budget for Nuclear Research of the Ministry of Education, Culture, Sports, Science, and Technology, based on the screening and counseling by the Atomic Energy Commission.

[1] G. Sposito and R. Prost, Chem. Rev. **82**, 353 (1982).
[2] A. Delville, Langmuir **7**, 547 (1991).
[3] G. Sposito and R. Prost, Chem. Rev. **82**, 554 (1982).
[4] D. A. Laird, Clays Clay Miner. **44**, 553 (1996).
[5] A. C. D. Newman, in *Chemistry of Clays and Clay Minerals* (Wiley, New York, 1987), pp. 1–128.
[6] N. Guven, in *Clay–Water Interface and its Rheological Implications*, edited by N. Guven and R. M. Pollastro (The Clay Mineral Society, Boulder, 1992), pp. 2–79.
[7] J. Cuadros, Am. J. Sci. **297**, 829 (1997).
[8] N. T. Skipper, Miner. Mag. **62**, 657 (1998).
[9] R. Prost, A. Koutit, A. Benchara, and E. Huard, Clay Miner. **46**, 117 (1998).
[10] B. J. Teppen, K. Resnussen, P. M. Bertsch, D. M. Miller, and L. Schafer, J. Phys. Chem. B **101**, 1579 (1997).
[11] R. M. Shroll and D. E. Smith, J. Chem. Phys. **111**, 9025 (1999).
[12] S. Kutter, J. P. Hansen, M. Sprik, and S. Boek, J. Chem. Phys. **112**, 311 (2000).
[13] A. Delville, J. Phys. Chem. **99**, 2033 (1995).
[14] E. S. Boek, P. V. Coveney, and N. T. Skipper, J. Am. Chem. Soc. **117**, 12608 (1995).
[15] F. R. C. Chang, N. T. Skipper, and G. Sposito, Langmuir **14**, 1201 (1998).
[16] G. Sposito, S. H. Park, and R. Sutton, Clays Clay Miner. **47**, 192 (1999).
[17] E. S. Boek, P. V. Coveney, and N. T. Skipper, Langmuir **11**, 4629 (1995).
[18] D. A. Laird, Clays Clay Miner. **47**, 4629 (1999).
[19] J. A. Greathouse, K. Refson, and G. Sposito, J. Am. Chem. Soc. **122**, 11459 (2000).
[20] R. F. Giese, Nature (London) **241**, 15 (1973).
[21] T. Ebina, T. Iwasaki, A. Chatterjee, M. Katagiri, and G. D. Stucky, J. Phys. Chem. B **101**, 1125 (1997).
[22] A. Chatterjee, T. Iwasaki, T. Ebina, and H. Hayashi, Appl. Surf. Sci. **121/122**, 167 (1997).
[23] A. Chatterjee, T. Iwasaki, H. Hayashi, T. Ebina, and K. Torri, J. Mol. Catal. A: Chem. **136**, 195 (1998).
[24] A. Chatterjee, T. Iwasaki, T. Ebina, and A. Miyamoto, Comput. Mater. Sci. **14**, 119 (1999).
[25] A. Chatterjee, T. Iwasaki, and T. Ebina, J. Phys. Chem. A **104**, 8216 (2000).
[26] V. Marry, P. Turq, T. Cartailler, and D. Levesque, J. Chem. Phys. **117**, 3454 (2002).
[27] R. G. Pearson, J. Am. Chem. Soc. **105**, 7512 (1983).
[28] R. G. Pearson, J. Chem. Educ. **64**, 561 (1987).
[29] R. G. Parr and W. Yang, J. Am. Chem. Soc. **106**, 4049 (1984).
[30] P. Geerlings and F. De Proft, Int. J. Quantum Chem. **80**, 227 (2000).
[31] L. T. Nguyen, T. N. Le, F. De Proft, A. K. Chandra, W. Langenaeker, M. T. Nguyen, and P. Geerlings, J. Am. Chem. Soc. **121**, 5992 (1999).
[32] W. Langenaeker, F. D. Proft, and P. Geerlings, J. Phys. Chem. A **102**, 5944 (1998).
[33] A. K. Chandra, P. Geerlings, and M. T. Nguyen, J. Org. Chem. **62**, 6419 (1997).
[34] D. Sivanesan, R. Amutha, V. Subramanian, B. U. Nair, and T. Ramaswami, Chem. Phys. Lett. **308**, 223 (1999).
[35] F. J. Luque, M. Orozco, P. K. Bhadane, and S. R. Gadre, J. Chem. Phys. **100**, 6718 (1994).
[36] F. J. Luque, S. R. Gadre, P. K. Bhadane, and M. Orozco, Chem. Phys. Lett. **232**, 509 (1995).
[37] R. G. Pearson and R. G. Parr, J. Am. Chem. Soc. **105**, 7512 (1983).
[38] W. Yang and M. J. Mortier, J. Am. Chem. Soc. **108**, 5708 (1986).
[39] M. P. Teter, M. C. Payne, and D. C. Allen, Phys. Rev. B **40**, 12255 (1989).
[40] M. C. Payne, M. P. Teter, D. C. Allan, T. A. Arias, and J. D. Johannopoulos, Rev. Mod. Phys. **64**, 1045 (1992).
[41] J. Perdew and A. Zunger, Phys. Rev. B **23**, 5048 (1981).
[42] B. Winkler, V. Milman, and M. C. Payne, Am. Mineral. **79**, 200 (1994).
[43] J. P. Perdew, Phys. Rev. B **33**, 8822 (1986).
[44] A. D. Becke, Phys. Rev. A **33**, 3098 (1988).
[45] K. Laasonen, F. Csajka, and M. Parrinello, Chem. Phys. Lett. **194**, 172 (1992).
[46] C. Lee, D. Vanderbilt, K. Laasonen, R. Car, and M. Parrinello, Phys. Rev. B **47**, 4863 (1993).
[47] A. Garcia, C. Elsasser, J. Zhu, S. G. Louie, and M. L. Cohen, Phys. Rev. B **46**, 9829 (1992).
[48] H. J. Monkhorst and J. D. Pack, Phys. Rev. B **13**, 5188 (1976).
[49] W. Kohn and L. J. Sham, Phys. Rev. A **140**, 1133 (1965).
[50] A. Becke, J. Chem. Phys. **88**, 2547 (1988).
[51] C. Lee, W. Yang, and R. G. Parr, Phys. Rev. B **37**, 786 (1988).
[52] C. W. Bock and M. Trachtman, J. Phys. Chem. **98**, 95 (1994).
[53] S. F. Boys and F. Bernardi, Mol. Phys. **19**, 553 (1970).
[54] A. Chatterjee, H. Hayashi, T. Iwasaki, T. Ebina, and K. Torii, J. Mol. Catal. A: Chem. **136**, 195 (1998).
[55] A. C. D. Newman and G. Brown, in *Minerological Society Monograph No. 5*, Chemistry of Clays and Clay Minerals, edited by A. C. D. Newman (Minerological Society, London, 1974), p. 10.
[56] P. F. Luckham and S. Rossi, Adv. Colloid Interface Sci. **82**, 43 (1999).
[57] C. H. Bridgeman, A. D. Buckingham, N. T. Skipper, and M. C. Pyne, Mol. Phys. **89**, 879 (1996).
[58] R. K. Roy, S. Krishnamurthy, P. Geerlings, and S. Pal, J. Phys. Chem. A **102**, 3746 (1998).
[59] A. Chatterjee, T. Iwasaki, and T. Ebina, J. Phys. Chem. A **105**, 10694 (2001).
[60] A. Chatterjee, T. Ebina, T. Iwasaki, and F. Mizukami, J. Chem. Phys. **118**, 10212 (2003).
[61] S. Stackhouse and P. V. Coveney, J. Phys. Chem. B **106**, 12470 (2002).
[62] E. S. Boek and M. Sprik, J. Phys. Chem. B **107**, 3251 (2003).